Modelling and simulation of the dynamic behaviour of a ball screw system using transmission line modelling technique

V.Y. Moreno-Castaneda, C. Pislaru, D.G. Ford, A.P. Longstaff, A. Myers
Centre for Precision Technologies, University of Huddersfield, UK

Abstract

This paper presents a new approach for the modelling of a screw shaft including the axial and torsional dynamics in the same model. The model includes the distributed parameter dynamics of the ball screw system and the effect of mass distribution. This is based on the flexibility of the Transmission Line Matrix Method (TLM) to develop lumped and distributed parameter systems. The procedure for the synchronisation of both axial and torsional effects is presented in detail.

1. Introduction

Various types of models for feed drives (lumped parameter models, modular approach, hybrid models) have been developed by industrial and academic researchers. However the simulated responses did not reflect entirely the overall dynamic behaviour of the machine tools because the stiffness calculations are made considering that the worktable is oscillating around one position.

A novel application of TLM for the modelling of the dynamic behaviour of Computer Numeric Controlled (CNC) machine tool feed drives for various running conditions was previously presented [1]. The considered feed drive was a non-linear hybrid system where the controller commanded the movement of a worktable linked to a motor through a ball-screw. This paper presents the improved TLM model of a ball-screw including the moving nut, the distributed inertia of the screw, the axial and torsional forces applied on the nut during its linear movement and the restraints applied by the bearings.

The application of TLM technique implies the division of the screw shaft into a large number of identical elements. This is necessary in order to achieve the synchronisation of events during simulation and produce acceptable resolution according to the maximum frequency of interest as presented by Beck et al [2].

This normally requires considerable computing effort when small time steps are used in the simulation process. This paper presents a solution to reduce the simulation time and calculation power and generate accurate and reliable results.

The TLM model is implemented in MATLAB and simulated values for different positions of the moving nut compare well with the measured data when same stimuli are applied to the model and the actual feed drive.

2. Transmission line matrix method

TLM is a numeric differential method usually used to solve problems of wave propagation through a medium. The system equations are made equivalent with the equations for voltages and currents for a mesh of transmission lines. TLM technique uses two circuits: The stub and the link.

Christopoulos [3] stated that any electrical circuit could be represented as a network of transmission sections by simply replacing the reactive components with corresponding stubs. Variables such as voltage and current are regarded as discrete pulses bouncing to and from the nodes of these stubs at each time step.

The voltage and current in each component (stub and link) is determined from the incident (E^i, A^i, B^i) and reflected (E^r, A^r, B^r) pulses in a port (Figure 1(a)). The TLM operation begins with the incident pulses representing the initial conditions being injected into the network. Incident pulses take a time (Δt) to travel between ports. When incident pulses reach a port (nodes), reflected pulses are generated according to boundary conditions. The reflected pulses thus become the incident pulses in the next time step. On incidence to the node, the pulse will interact with other parts of the circuit.

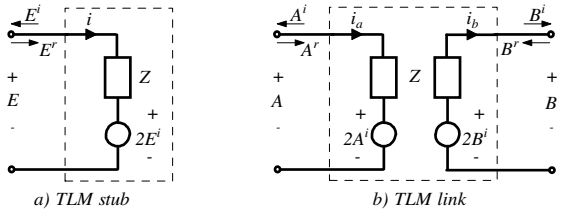

a) TLM stub *b) TLM link*

Figure 1: TLM Units

If $E^i(k)$ is known at time step k, the voltages and current in Figure 1(a) may be calculated. Taking $E^i(k)$ as the discrete stimulus applied to the stub, gives:

$$i(k) = (E(k) - 2E^i(k))/Z \tag{1}$$

the reflected pulse will be $$E^r(k) = E(k) - E^i(k) \tag{2}$$

the reflected pulse becomes the next incident pulse, hence

$$E^i(k+1) = \Gamma * E^r(k) \tag{3}$$

Now, with $E^i(k+1)$ obtained from eqn (4), i($k+1$) may be obtained from eqn (1). Then, the process (scattering algorithm) is repeated for as long as desired. The characteristic impedance Z and the reflection factor Γ are chosen accordingly to the nature of the element to be represented.

The application of the scattering algorithm to the TLM link gives:

$$i_a(k) = (A(k) - 2A^i(k))/Z \qquad i_b(k) = (B(k) - 2B^i(k))/Z \tag{5}$$

$$A^r(k) = A(k) - A^i(k) \qquad B^r(k) = B(k) - B^i(k) \tag{6}$$

the reflected pulses become the next incident pulses, hence

$$A^i(k+1) = B^r(k) \qquad B^i(k+1) = A^r(k) \tag{7}$$

Eqns (5) to (7) represent the TLM link algorithm, which is a numerical method for the solution of the wave equation (Sadiku and Agba [4]) with the form:

$$\frac{1}{C}\frac{\partial^2 y(x,t)}{\partial x^2} = L\frac{\partial^2 y(x,t)}{\partial t^2} \tag{8}$$

Where the velocity of propagation (u) and the impedance (Z) are:

$$u = \sqrt{(1/C)/L} \qquad Z = \sqrt{L/C} \tag{9}$$

C and L are the capacitance and inductance per unit length of a transmission line. The function $y(x,t)$ can represent either voltage or current on the transmission line.

Partidge et al [5] used this concept to model a shaft and turntable with linear and non-linear friction. TLM stubs represented lumped elements (turntable inertia), and distributed elements (shaft) were modelled by TLM links. Thus, for the equation for torsional vibration of a shaft

$$G_m J_m(\partial^2 y(x,t)/\partial x^2) = \rho_m J_m(\partial^2 y(x,t)/\partial t^2) \tag{10}$$

The function $y(x, t)$ signifies either torque or angle of twist. The velocity of propagation u_t and the impedance Z_t for the equivalent TLM link are:

$$u_t = \sqrt{G_m/\rho_m} \tag{11}$$

$$Z_t = \rho_m G_m u_t \tag{12}$$

G_m, J_m, ρ_m, E_m and A_m represent respectively: the material rigidity modulus, the polar moment of inertia, the material density, the material Young's modulus, and the cross sectional area of the shaft.

The same method can be applied for the equation of the longitudinal vibration of a bar - eqn (15), where the parameters of the equivalent TLM link are:

$$u_a = \sqrt{E_m/\rho_m} \tag{13}$$

$$Z_a = \rho_m A_m u_a \tag{14}$$

$$E_m A_m(\partial^2 y(x,t)/\partial x^2) = \rho_m A_m(\partial^2 y(x,t)/\partial t^2) \tag{15}$$

The function $y(x, t)$ represents either axial force or longitudinal displacement.

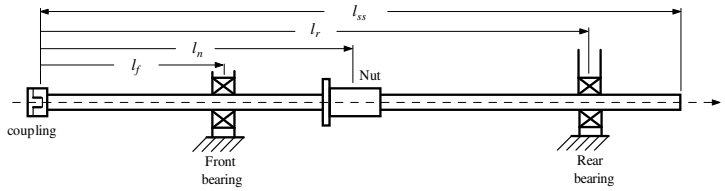

Figure 2: Ball screw arrangement

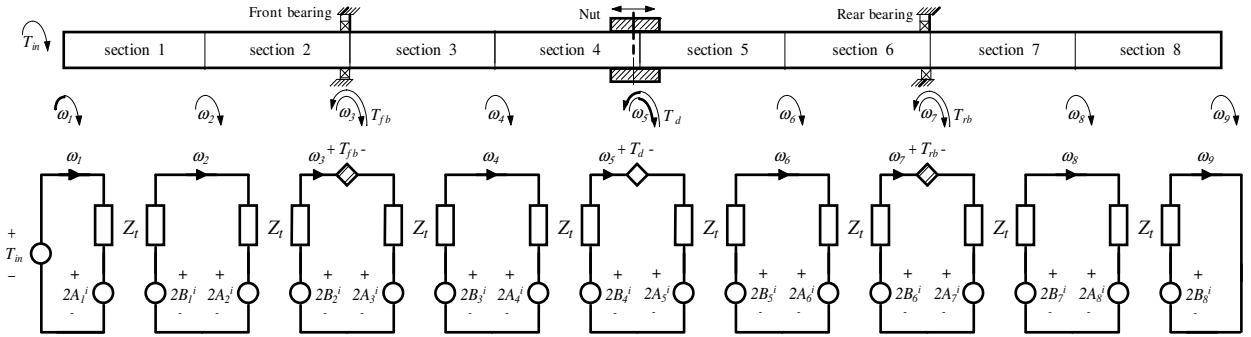

Figure 3: TLM model of a shaft divided into eight sections including supporting bearings friction and moving nut

j	1	2	3	4	5	6	7	8
ω_j	$\frac{T_{in}-2A_1^i}{Z_t}$	$\frac{2(B_1^i-A_2^i)}{2Z_t}$	$\frac{2(B_2^i-A_3^i)-T_{fb}}{2Z_t}$	$\frac{B_3^i-A_4^i}{Z_t}$	$\frac{2(B_4^i-A_5^i)-T_d}{2Z_t}$	$\frac{B_5^i-A_6^i}{Z_t}$	$\frac{2(B_6^i-A_7^i)-T_{rb}}{2Z_t}$	$\frac{B_7^i-A_8^i}{Z_t}$
A_j^r	$\omega_1 Z_t + A_i^i$	$\omega_2 Z_t + A_2^i$	$\omega_3 Z_t + A_3^i$	$\omega_4 Z_t + A_4^i$	$\omega_5 Z_t + A_5^i$	$\omega_6 Z_t + A_6^i$	$\omega_7 Z_t + A_7^i$	$\omega_8 Z_t + A_8^i$
B_j^r	$B_1^i - \omega_2 Z_t$	$B_2^i - \omega_3 Z_t$	$B_3^i - \omega_4 Z_t$	$B_4^i - \omega_5 Z_t$	$B_5^i - \omega_6 Z_t$	$B_6^i - \omega_7 Z_t$	$B_7^i - \omega_8 Z_t$	$B_8^i - \omega_9 Z_t$

$B_j^i(k+1) = A_j^r$ and $A_j^i(k+1) = B_j^r$, then when substituting ω_j into the equation for A_j^r gives:

$B_j^i(k+1)$	$T_{in} - A_1^i$	B_1^i	$\omega_3 Z_t + A_3^i$	B_3^i	$\omega_5 Z_t + A_5^i$	B_5^i	$\omega_7 Z_t + A_7^i$	B_7^i
$A_j^i(k+1)$	A_2^i	$B_2^i - \omega_3 Z_t$	A_4^i	$B_4^i - \omega_5 Z_t$	A_6^i	$B_6^i - \omega_7 Z_t$	A_8^i	$-B_8^i$

Table 1: Calculation of angular velocities and incident pulses for the TLM model of Figure 3

3. TLM model for the ball screw system

The screw shaft is mounted on two preloaded bearings as shown in Figure 2. The positions of the front bearing (l_f), rear bearing (l_r) and nut (l_n) are defined taking as a reference the screw end attached to the coupling.

The screw shaft is divided into eight sections (Figure 3) as an example of the TLM model for the torsional dynamics of the shaft. The front bearing is placed on section two, the nut is on section four and the rear bearing is on section six. Table 1 contains the equations for each shaft section according to the TLM link scattering algorithm. The angular speed at the last section is calculated as

$$\omega_9 = 2B_8^i / Z_t \tag{16}$$

It can be seen that pulses are propagated through out the shaft until a disturbance is present in the system. The input torque T_{in} in the first section, the frictional torque in the front bearing (T_{fb} on section two), the torque needed to counterbalance the effect of the table (T_d on section four), the frictional torque in the rear bearing (T_{rb} on section six), and the end of the shaft on the last section. Incident pulses are reflected at those points according to the boundary conditions. This dynamic behaviour resembles a circular (linked) list where information is stored to be analysed and modified at designated positions. Thus, the propagation of pulses in the TLM model takes place on three specific zones (loops) as it is graphically represented in Figure 4.

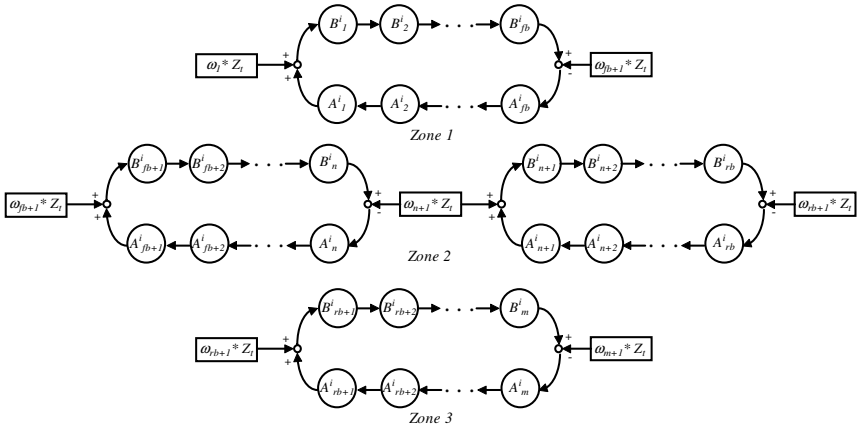

Figure 4: Pulse propagation model for the screw shaft torsional dynamics

The same approach is applied for the TLM axial model of the screw shaft. This leads to the propagation of pulses on three specific zones (loops) in the axial model as it is graphically represented in Figure 5. The screw shaft is divided into m_a sections, the front bearing is placed on the section fb_a, the nut is on the section n_a and the rear bearing is on the section rb_a, where:

$$fb_a = \mathrm{mod}(l_f / m_a - 0.5) \tag{17}$$

$$n_a = \mathrm{mod}(l_n / m_a - 0.5) \tag{18}$$

$$rb_a = \mathrm{mod}(l_r / m_a - 0.5) \tag{19}$$

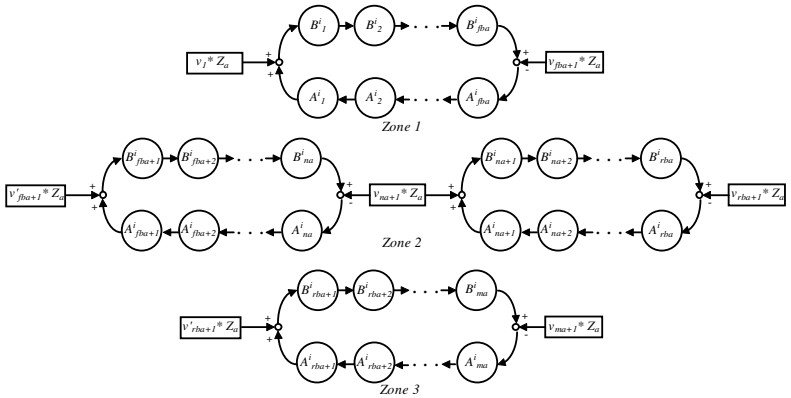

Figure 5: Pulses propagation model for the screw shaft torsional dynamics

The model is reduced to the calculation of the longitudinal velocity on section one, fb_a, rb_a, n_a, and m_a; and the propagation of pulses on the other sections.

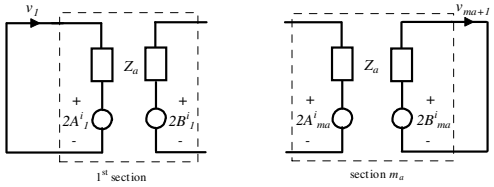

Figure 6: First and last section of the TLM axial model for the screw shaft

The velocities on the first section (v_1) and the last section (v_{ma+1}) are calculated from the circuits illustrated in Figure 6 as:

$$v_1 = -2A_1^i(k)/Z_a \qquad v_{ma+1} = 2B_{ma}^i(k)/Z_a \tag{20}$$

Next pulses: $$B_1^i(k+1) = -A_1^i(k) \qquad A_{ma}^i(k+1) = -B_{ma}^i(k) \tag{21}$$

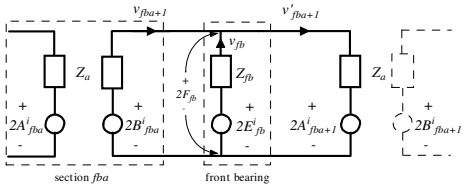

Figure 7: Section fb_a of the TLM axial model for the screw shaft

The force applied to the front bearing mounting ($2F_{fb}$) and its velocity (v_{fba}) are calculated including the TLM model for the stiffness of the front bearing mounting (see Figure 7):

$$F_{fb} = (1/(2Z_{fb} + Z_a)) * (Z_{fb} * (B_{fba}^i + A_{fba+1}^i) + Z_a * E_{fb}^i) \tag{22}$$

$$v_{fba+1} = 2 * (B_{fba}^i - F_{fb})/Z_a \qquad v'_{fba+1} = 2 * (F_{fb} - A_{fba+1}^i)/Z_a \tag{23}$$

$$v_{fb} = v'_{fba+1} - v_{fba+1} \tag{24}$$

Next pulses: $$E^i_{fb}(k+1) = 2 * F_{fb} - E^i_{fb}(k) \quad (25)$$

$$A^i_{fba}(k+1) = B^i_{fba}(k) - v_{fba+1} * Z_a \qquad B^i_{fba+1}(k+1) = A^i_{fba+1}(k) + v'_{fba+1} * Z_a \quad (26)$$

Where, $$Z_{fb} = (t_a / 2) * k_{fb} \quad (27)$$

t_a and k_{fb} in eqn (32) represent respectively: the propagation time on a section of the axial model and the stiffness of the front bearing mounting.

Applying the same configuration to the section rb_a gives (k_{fb} represents the stiffness of the rear bearing mounting):

$$F_{rb} = (1/(2Z_{rb} + Z_a)) * (Z_{rb} * (B^i_{rba} + A^i_{rba+1}) + Z_a * E^i_{rb}) \quad (28)$$

$$v_{rba+1} = 2 * (B^i_{rba} - F_{rb}) / Z_a \qquad v'_{rba+1} = 2 * (F_{rb} - A^i_{rba+1}) / Z_a \quad (29)$$

Next pulses: $$E^i_{rb}(k+1) = 2 * F_{rb} - E^i_{rb}(k) \quad (30)$$

$$A^i_{rba}(k+1) = B^i_{rba}(k) - v_{rba+1} * Z_a \qquad B^i_{rba+1}(k+1) = A^i_{rba+1}(k) + v'_{rba+1} * Z_a \quad (31)$$

Where, $$Z_{rb} = (t_a / 2) * k_{rb} \quad (32)$$

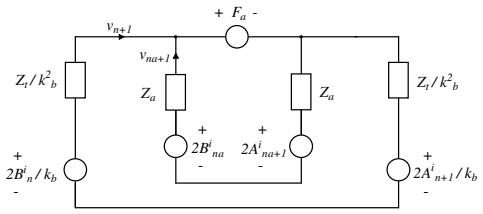

Figure 8: Connection between the torsional and axial TLM models

Velocities ω_{n+1} and v_{na+1} are calculated analysing the connection between the axial and torsional models of the screw shaft, as shown in Figure 8. For this purpose, the variables of the torsional model on section n are converted using the ball screw force to torque conversion factor (k_b), thus:

$$v_{n+1} = ((2 * (B^i_n - A^i_{n+1}) / k_b) - F_a) / (2Z_t / k^2_b) \quad (33)$$

$$v_{na+1} = (2 * (B^i_{na} - A^i_{na+1}) - F_a) / (2Z_a) \quad (34)$$

Where, $$F_a = T_d / k_b \quad (35)$$

$$\omega_{n+1} = v_{n+1} / k_b \quad (36)$$

$$B^i_{na+1}(k+1) = A^i_{na+1}(k) + v_{na+1} * Z_a \qquad A^i_{na}(k+1) = B^i_{na}(k) - v_{na+1} * Z_a \quad (37)$$

The propagation on the other sections:

$$B^i_j(k+1) = B^i_{j-1}(k) \quad \text{for } j = 2,\ldots, m_a \;\; j \neq fb_a+1, n_a+1, rb_a+1 \quad (38)$$

$$A^i_j(k+1) = A^i_{j+1}(k) \quad \text{for } j = 1,\ldots, m_a-1 \;\; j \neq fb_a, n_a, rb_a \quad (39)$$

4. Synchronisation between torsional and axial models

The application of TLM theory to the modelling of the screw shaft gives different propagation velocities for the torsional and axial models (see eqns (11) and (13)). This leads to different torsional and axial propagation times (t_t, t_a) for the same section length. The synchronisation between axial and torsional models

can be achieved using the ratio between axial and torsional propagation speeds as follows:

$$\frac{u_a}{u_t} = \sqrt{\frac{E_m}{G_m}} = \frac{n_a}{n_t} \tag{40}$$

This value means that the time spent by an axial wave travelling n_a sections is equal to the time spent by a torsional wave travelling on n_t sections (where n_a and n_t are integers). To model this effect, each torsional section is dived into n_t axial sections to assure that axial and torsional pulses are arriving to the same point at the same time. Subsequently the number of sections of the axial model (m_a) will be n_t times the number of sections in the torsional model (m), hence

$$m_a = n_t * m \tag{41}$$

The propagation time of the axial waves is then calculated as:

$$t_a = \frac{n_t}{n_a} t_t \tag{42}$$

The application of this procedure using the values for G_m and E_m specified for steel gives a ratio

$$n_a / n_t = \sqrt{206/79.6} = 1027/638 = 1.6097 \tag{43}$$

This ratio implies to evaluate the axial model 1027 times per every simulation of the torsional model, if each section of the torsional model contains 638 sections of the axial model. This value can be reduced to speed up the simulation by analysing a variation of 1% in the values of the parameters G_m and E_m as shown in Table 2.

	$1.01*E_m$	$0.99*E_m$
$1.01*G_m$	1.6087	**1.5927**
$0.99*G_m$	**1.6249**	1.6087

Table 2: n_a/n_t ratio for variations of 1% in the values of G_m and E_m

It can be assumed from Table 2 that a ratio between 1.5929 and 1.6246 is valid taking into account the variations the screw shaft material may have due to the fabrication process. Therefore, the minimum rational number found into this interval (8/5) is selected for the modelling process (n_t = 5). In these conditions, E_m is approximated to $204.8 \text{x} 10^9$ N/m^2 for a given value of $G_m = 80 \text{x} 10^9$ N/m^3.
The length of each section in the torsional model (l_{tor}) and m will be:

$$l_{tor} = t_{pwm} * u_t \tag{44}$$

$$m = l_{ss} / l_{tor} \tag{45}$$

If m is not an integer number, it is rounded to the nearest integer. This implies to change the length of the screw shaft by certain quantity. Applying this procedure for l_{ss} = 1.346 m and t_t = 1 μs, gives:

$$u_t = \sqrt{80x10^9 / 7850} = 3192.3 \text{ [m/s]} \tag{46}$$

$$l_{tor} = 1x10^{-6} * 3192.3 = 3.1923x10^{-3} \text{ [m]} \tag{47}$$

$$m = 1.346 / 3.1923x10^{-3} = 421.63 \approx 422 \text{ sections} \tag{48}$$

This means, an increase in the length of the screw shaft (l_{ss}) of:

$$(422 - 421.03) * 3.1923x10^{-3} = 117.06\ \mu m \tag{49}$$

This error model could be present in the real system due to the tolerances in the machining process of the shaft and changes in the values of the physical properties of the material. For example, if the density value is changed by 0.63% to 7800, the number of sections will be 420 and the length of the screw shaft will be reduced by 92.35 μm.

An approach to cope with this limitation of the modelling technique is to assume that the density of the material could vary 1% its nominal value. In consequence, a valid number of sections can be defined (without altering the length of the shaft) by rounding the value of m towards minus infinity. Then:

$$m = 1346/3.1923 = 421.63 \approx 421 \text{ sections} \tag{50}$$

The number of sections of the axial model will be

$$m_a = 5 * 421 = 2105 \text{ sections} \tag{51}$$

Rearranging eqn (44) gives:

$$l_{tor} = l_{ss} / m = 1346/421 = 3.1971 \text{ [mm]} \tag{52}$$

$$u_t = l_{tor} / t_t = 3.1971x10^{-3} / 1x10^{-6} = 3197.15 \text{ [m/s]} \tag{53}$$

$$\rho_{ss} = \frac{G_{ss}}{u_t^2} = \frac{80x10^9}{(3197.15)^2} = 7826.43 \text{ [kg/m}^3\text{]} \tag{54}$$

The torsional impedance is calculated using eqn (12):

$$Z_t = 1.97x10^{-3} * 3197.15 = 6.29 \tag{55}$$

The propagation time for the axial model is

$$t_a = \frac{5}{8} * 1x10^{-6} = 6.25x10^{-7} \text{ [s]} \tag{56}$$

u_a can be calculated from eqn (40) as:

$$u_a = \frac{n_a}{n_t} * u_t = \frac{8}{5} * 3197.15 = 5115.44 \text{ [m/s]} \tag{57}$$

The axial impedance is calculated using eqn (14):

$$Z_a = \rho_{ss} * A_{ss} * u_a = 7826.43 * 9.13x10^{-4} * 5115.44 = 36563.32 \tag{58}$$

The length of each axial section is given by

$$l_{axial} = l_{tor} / 5 \tag{59}$$

5. Comparison between simulated and measured results

Figure 9 shows the measured and simulated frequency spectrum of the velocity control loop (impulse response). Measured results were obtained from the controller's oscilloscope through software provided by the manufacturer for the diagnosing of digital control loops. Simulations were conducted using specially written MATLAB code.

Analysing the measured and simulate results reveals that the TLM model is predicting the system's main oscillating frequency (at around 338 Hz) however the peaks in the simulated diagram are slightly displaced and are more difficult

to distinguish.
Although the results demonstrate the accuracy of the TLM model in resembling the dynamic behaviour of the ball screw system, more research needs to be done in order to improve the model.

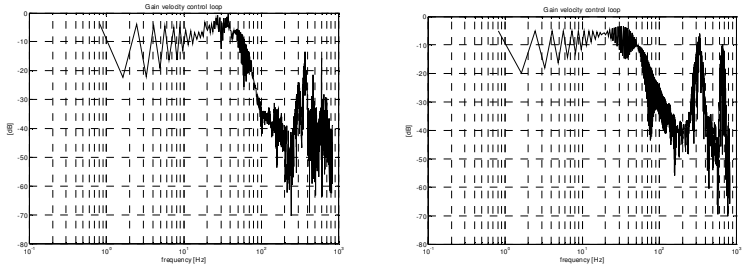

a) Measured b) Simulated

Figure 9: Frequency spectrum of the ball screw velocity control loop

6. Conclusions

The paper presents an approach for the TLM modelling of a screw shaft including the axial and torsional dynamics in the same model. This was accomplished by deriving a procedure for the synchronisation of both axial and torsional effects. In this regard, it was assumed that the physical properties of the screw shaft material (density) could vary with 1% its nominal value.

The simulated results compare well with the measured data when same stimuli are applied to the model and the actual feed drive.

The TLM method is faster and mathematically attractive avoiding becoming too involved in the boundary value problems associated with partial differential equations.

Future research will concentrate in using TLM for developing accurate feed drives models, which could become part of automatic tuning and condition-monitoring methods.

References

[1] Moreno-Castaneda, VY, Pislaru, C, Freeman, JM, Ford, DG, *Modelling and simulation of a feed drive using the transmission line modelling technique*, Proceedings of LAMDAMAP 2003, pp. 193-204, 2003.

[2] Beck SM, Haider, H, Boucher, RF, *Transmission line modelling of simulated drill strings undergoing water hammer*, Proceedings of IMecE, Journal of Mechanical Engineering Science Vol. 209, pp. 419-427, 1995.

[3] Christopoulos C, *The Transmission-line modeling method TLM*, IEEE Press, New York, USA , 1995.

[4] Sadiku, MNO, Agba, LC, *A simple introduction to the transmission line modeling,* IEEE Transactions on Circuits and Systems, Vol. 31, No. 8, pp 991-999, 1990.

[5] Partridge, GJ, Christopoulos, C, and Johns, PB, *Transmission line modelling of shaft system dynamics*, Proceedings of IMecE, Part C, Journal of Mechanical Engineering Science, Vol. 210, No. 4, pp. 271-278, 1987.